ACS Sustainable Chemistry & Engineering

Letter

Cite This: ACS Sustainable Chem. Eng. 2018, 6, 12580−12585

pubs.acs.org/journal/ascecg

Porous Polyethylene Bundles with Enhanced Hydrophobicity and Pumping Oil-Recovery Ability via Skin-Peeling

Xudong Zhang,[†,‡] Xiaolong Wang,[†] Xianhu Liu,[*,†] Cunjing Lv,[§] Yaming Wang,[†] Guoqiang Zheng,[†] Hu Liu,[†,‡] Chuntai Liu,[†] Zhanhu Guo,[‡,∥] and Changyu Shen[†]

[†]Key Laboratory of Materials Processing and Mold, Ministry of Education, National Engineering Research Center for Advanced Polymer Processing Technology, Zhengzhou University, No. 97-1 Wenhua, Jinshui District, Zhengzhou 450002, China

[‡]Integrated Composites Laboratory (ICL), Department of Chemical & Biomolecular Engineering, University of Tennessee, 1015 Volunteer Boulevard, Knoxville, Tennessee 37996, United States

[§]Department of Engineering Mechanics, Tsinghua University, No. 1 Qinghuayuan, Haidian District, Beijing 100084, China

[∥]College of Chemical and Environmental Engineering, Shandong University of Science and Technology, 579 Qianwangang, Qingdao, Shandong 266590, China

Supporting Information

ABSTRACT: Developing a feasible and efficient adsorption material for the large area of an oil leak is still challenging due to the critical limitation of complex production process and expensive cost. In this work, the tridimensional interconnected porous high-density polyethylene bundles based on the immiscible polymer blend principle were successfully fabricated via melt extrusion and water leaching method. However, due to the hydrophilicity of polyethylene, the porous bundles featured modest hydrophobicity with a water contact angle about 97° ± 2.8° and low efficiency of oil recovery. To achieve good hydrophobicity, we present a skin-peeling route for forming an enhanced hydrophobic surface. After skin-peeling, due to the existence of villus-like fiber structure, the bundle surfaces showed excellent hydrophobicity with a water contact angle of 139° ± 4.8°, as well as the strong lipophilicity and pumping oil-recovery ability, endowing the materials with potential applications in continuous oil−water separation. This work proposes not only an efficient and green way to fabricate porous polyethylene bundles with enhanced hydrophobicity and pumping oil-recovery ability but also a new opportunity for potential commercial applications.

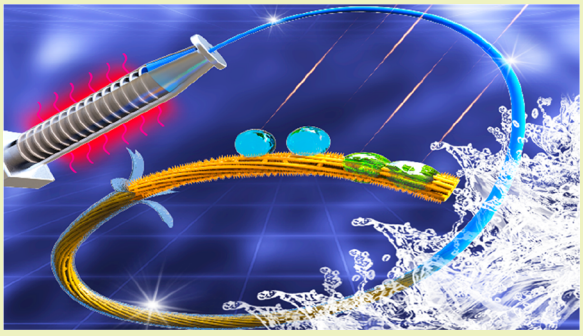

KEYWORDS: *Adsorption material, Hydrophobicity, Polyethylene, Oil−water separation*

INTRODUCTION

With continuous development of the offshore oil exploitation and oil transportation, oil spills have occurred too many times in this world, which has become an urgent global environmental issue. So far, various approaches have been developed including combustion, sorbents, skimmers, bioremediation, chemical dispersion, and filtration.[1−4] However, the mentioned methods suffer from either low separation efficiency, secondary contamination or discontinuous separation. Considering this, many efforts have been devoted to develop advanced porous materials (monoliths) by creating micro/nano structures on their surface via improve surface roughness,[5−7] which usually possess contrasting wettability toward water and oil, and therefore endow selective oil/water adsorption.

Polyolefin, a class of important commodity plastic, has a considerable commercial importance due to its good comprehensive properties, such as low cost, good processability, high ductility and impact strength.[8−10] Therefore, many researches focus to develop polyolefin based new materials with desired performance in view of its commercial importance.[11−15] For example, some simple and inexpensive methods for forming a superhydrophobic surface based on polypropylene and polyethylene have been proposed.[13−15] However, most of these promising materials still have some limitations for could not be combined with present commercial techniques such as the manufacturing of polyolefin fiber by extrusion.

Up to now, many attempts to mimic lotus leaf have achieved great progress; however, a simple and economical procedure still remains to be found. Polymer extrusion, which is produced more than 40% of plastic products, is one of the basic methods in polymer processing due to its simple operation and continuous production with automatization capacity.[15−17] Lotus leaf surface possesses superhydrophobic because of its villi structure. If we can make the materials with villi structure via extrusion method similar to the lotus leaf surface, the porous polyolefin bundles with hierarchical structure and superhydrophobicity would be

Received: July 11, 2018
Revised: July 29, 2018
Published: September 4, 2018

DOI: 10.1021/acssuschemeng.8b03305
ACS Sustainable Chem. Eng. 2018, 6, 12580−12585

Scheme 1. Illustration for the Fabrication of Peeled Porous HDPE Bundles (P3Bs) and Their Application

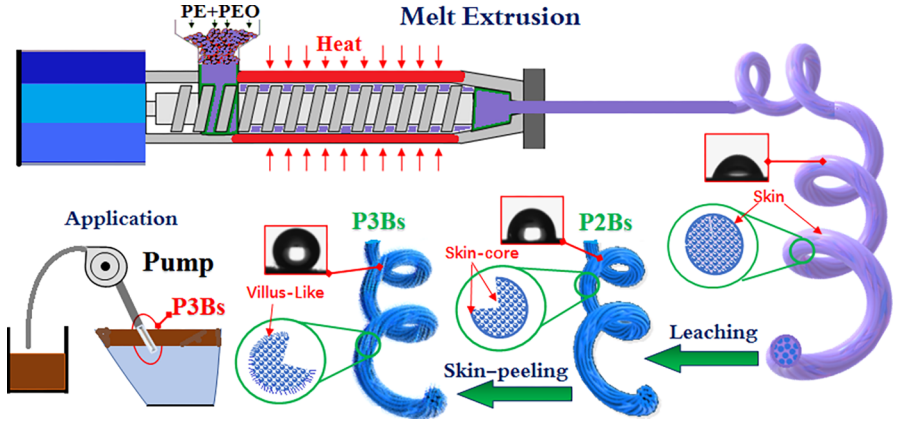

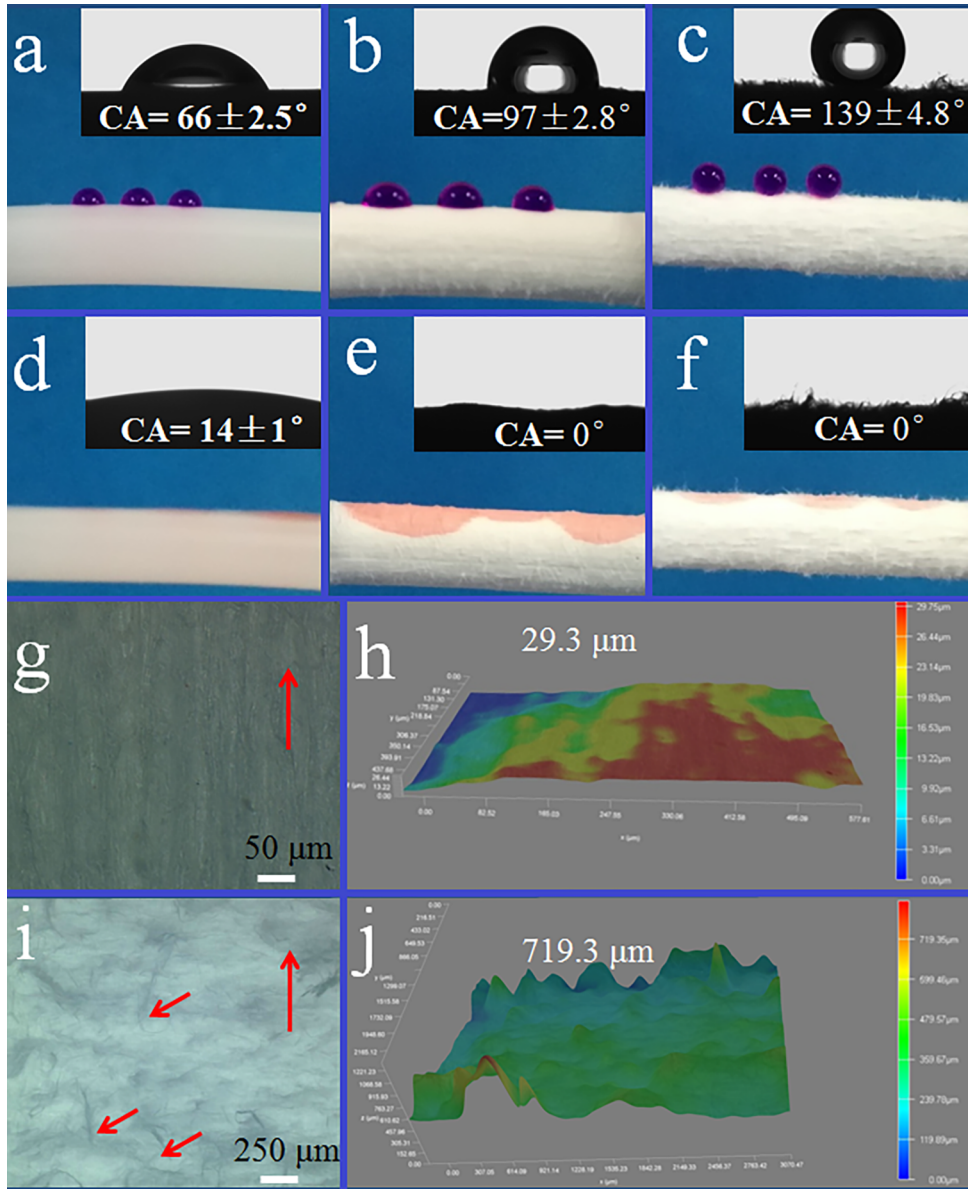

Figure 1. Contact angle of (a−c) water and (d−f) cyclohexane droplets on the (a, d) P1Bs, (b, e) P2Bs and (c, f) P3Bs as well as (g, i) plan views and (h, j) 3D views of surface images of (g, h) P2Bs and (i, j) P3Bs.

obtained in large scale. Based on this idea, the tridimensional interconnected porous high-density polyethylene (HDPE) bundles were fabricated via melt extrusion and leaching method. We have attempted to create villi structure on the porous HDPE

DOI: 10.1021/acssuschemeng.8b03305
ACS Sustainable Chem. Eng. 2018, 6, 12580−12585

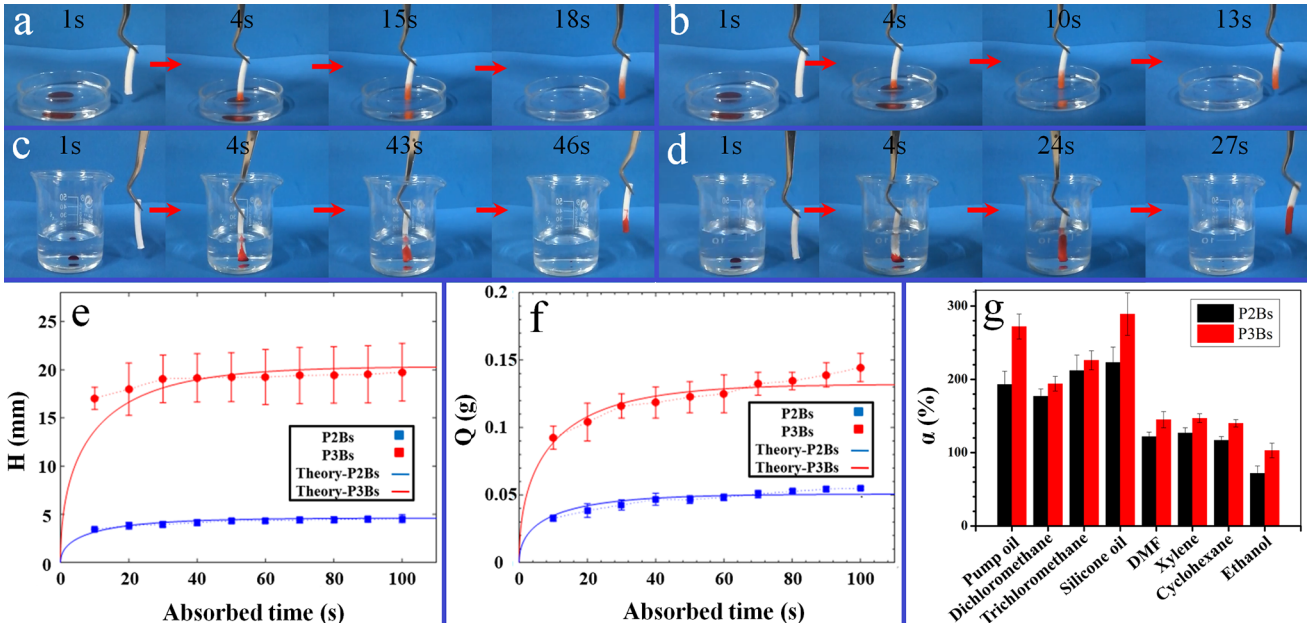

Figure 2. Oil/water separation capacity: Removal process of (a, b) cyclohexane on water and (c, d) chloroform underwater for (a, c) P2Bs and (b, d) P3Bs. Comparisons: (e) absorption height H and (f) oil-absorption quality Q of P2Bs and P3Bs as functions of time between the theoretical and experimental results. (g) Mass absorption capacities α of the P2Bs and P3Bs for various organic solvents and oils.

bundle surface by employing skin-peeling, and then compared the two kinds of porous HDPE bundles and determined the peeled bundle that exhibits enhanced hydrophobicity and lipophilicity.

EXPERIMENTAL SECTION

Preparation of Peeled Porous HDPE Bundles. The fabrication of the peeled porous HDPE bundles (P3Bs) is illustrated in Scheme 1. The HDPE/poly(ethylene oxide) (PEO) (50/50 wt %) blend was melt mixed via a mini twin-screw extruder (SJZS-10A, Wuhan Ruiming Plastic and Mechanical Co., Ltd.) with a screw rotation speed of 10 rpm at 150 °C. To create villi structure on the surface of HDPE bundles, a temperature gradient method was introduced. Therefore, the obtained HDPE/PEO extrudates have a skin-core structure,[18] which is like the skin-core structure of injection-molded parts.[19−21] The HDPE/PEO extrudates were extracted in deionized water and ultrasonic cleaned by an ultrasonic cleaner for 8 h at room temperature and the deionized water was changed every 30 min. After extraction, the specimens were first frozen in a refrigerator for 12 h at −17 °C, and then freeze-dried at −70 °C for 48 h. The obtained porous HDPE (P2Bs) can be easily skin-peeled by tweezers (Figure S1), and therefore the P3Bs with villus-like structure were fabricated. For comparison, pure HDPE (P1Bs) was also prepared under the same processing conditions.

Characterization. Water and oil contact angle (CA) measurements were implemented on a contact angle goniometer (SL200 KS, KINO, USA). The averaged CA was obtained from at least five measurements. The surface morphology was characterized by using a LEICA DVM6 optical microscopy instrument. Specimens with lengths of 30 and 10 mm were used for oil-absorption measurements and pumping collection, respectively. Saturated adsorption capacity was defined as percentage of grams of oil or organic solvent adsorbed per gram of sample (g/g × 100) and calculated by the following equation:

$$\alpha(\%) = \frac{(m_e - m_o)}{m_o} \times 100 \quad (1)$$

where m_o and m_e are the absorb materials weights before and after absorption test, respectively. In order to explore the variation of the porosity of P2Bs before and after peeling, ethanol saturation method was used. The calculated porosity increased from 43% for P2Bs to 52% for P3Bs, indicating the porosity of the samples increases after peeling treatment.

RESULTS AND DISCUSSION

Contact Angle and Surface Morphology. Figure 1 shows the contact angle and surface morphology of P2Bs and P3Bs. As shown in Figure 1a−c, water drop with a CA of 66 ± 2.5°, 97 ± 2.8° and 139 ± 4.8° on the surface of P1Bs, P2Bs and P3Bs was obtained, respectively, indicating an enhanced hydrophobicity. The P1Bs surface with an oil CA of 14 ± 1° (Figure 1d), whereas the P2Bs (Figure 1e) and P3Bs (Figure 1f) with an oil CA of 0°. Apparently, the contact area (spreading area) of P2Bs is larger than the P3Bs. Herein, one may say that the wettability of P2Bs is better than P3Bs. However, the roughness of P3Bs is larger than P2Bs, so P3Bs should be more lipophilic. Due to some villi distributed vertically along the surface, it will block the oil to spread and absorbed fast into the bundle. Therefore, the oil wettability of P3Bs is better than that of P2Bs. The described results indicate that the P3Bs possess excellent hydrophobicity and lipophilicity.

The existence of interconnected microchannels in P2Bs increases surface roughness (Figure S2), and surface roughness contributes significantly to enhancing liquid repellence.[13] The surface of P2Bs is relatively smooth with a height difference of 15.4 μm (Figure 1h). After peeling, the special villus-like structure that has orientation under external force was formed and the P3Bs with topographic surface was obtained (Figure 1i). The height difference of P3Bs is augmented to 719.3 μm (Figure 1j). According to the Wenzel and Cassie−Baxter model, the introduction of an appropriate multiscale roughness could improve the hydrophobicity. Therefore, the water CA of the P3Bs surface is larger than that of P2Bs.

Both P2Bs and P3Bs showed higher surface hydrophobicity than the P1Bs. This can be explained by Cassie's composite contact theory. According to the classical theories, the apparent CA, θ, can be given as the functions of the geometric parameters of the microstructures on the surface:

DOI: 10.1021/acssuschemeng.8b03305
ACS Sustainable Chem. Eng. 2018, 6, 12580−12585

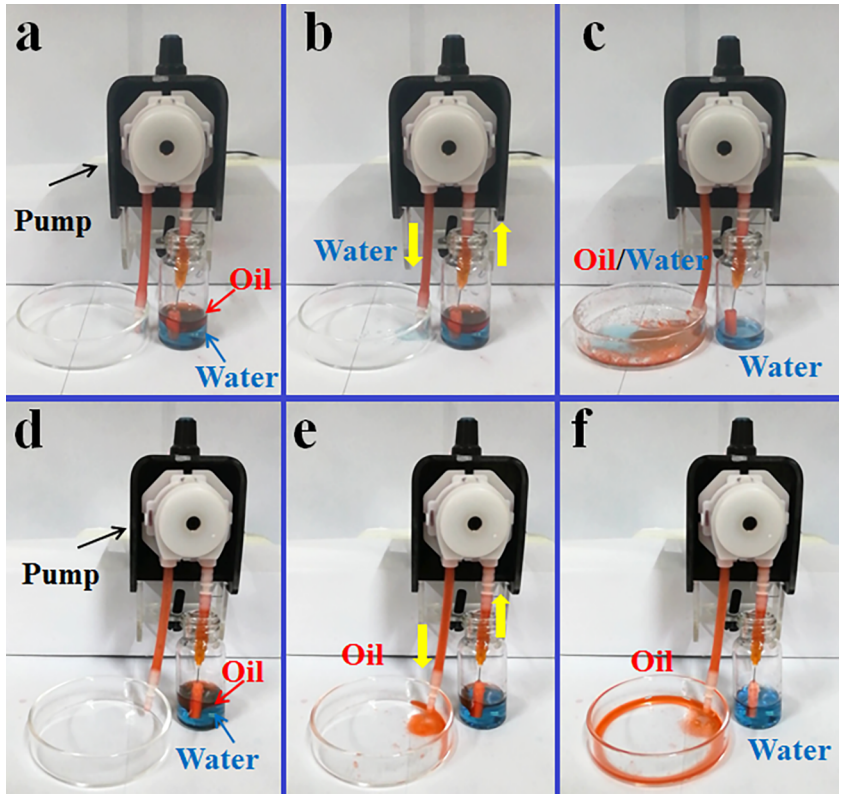

Figure 3. Photographs of continuous pumping collection of cyclohexane from water used P2Bs (a–c) and P3Bs (d–f). Cyclohexane and water were respectively dyed with Sudan III and methylene blue for clear observation.

$$\cos\theta = f\cos\theta_0 + f - 1 \quad (2)$$

where θ_0 is the intrinsic CA of the smooth HDPE surface, and f is the surface fraction, which is defined as the ratio of the solid–liquid contact area to the apparent droplet contact area on the solid surface. The f values were estimated as 0.69 and 0.18 for P2Bs and P3Bs, respectively (Figure 1). Considering $\theta_0 = 66°$, so the calculated CAs in Cassie wetting state were 92° and 137°, respectively, which is in good agreement with the corresponding experimental results of 97 ± 2.8° and 139 ± 4.8°.

Oil–Water Separation and Modeling of Oil Adsorption. Due to hydrophobicity and superlipophilicity, P3Bs have great potential for oil/water separation. The separation processes for insoluble oil from oil/water mixture are shown in Figure 2. The cyclohexane and chloroform were immediately taken up when the porous bundles got closed to it. The completely adsorbed cyclohexane and chloroform time of P3Bs are 13 s (Figure 2b and Movie S3) and 27 s (Figure 2d and Movie S4), respectively. In contrast, for P2Bs, they are respectively 18 s (Figure 2a and Movie S1) and 46 s (Figure 2c and Movie S2).

Figure 2e,f displays the weight gain of oil and the absorption height as a function of time. Overall, the adsorption quality increased as time for both porous bundles, and P3Bs have faster oil absorption rate compared with P2Bs, but the oil absorption height has made little change. Nevertheless, the adsorption quality of P3Bs is 3 times heavier than P2Bs, and the absorption height of P3Bs reaches 20 mm whereas that of P2Bs is only 4 mm. These results imply that the P3Bs has a better oil absorption efficiency than P2Bs.

The absorption of the oil in the fiber is driven by the capillary force, i.e., $2\sigma\cos\theta/r_{equ}$, denoting σ and r_{equ} the oil–air surface tension and the equivalent radius of the pores in the fiber, respectively. The drag force mainly comes from the viscous force during the transport of the oil liquid,[22] i.e., $\varepsilon\mu hU/K$, where ε and K are the material porosity and the permeability the fiber. μ is the viscosity of the oil. H and U are the height of the front edge of the oil and its corresponding velocity, which indicates $U = dH/dt$, denoting t the time. Since the rise height of the oil is obviously larger than the capillary length (see Figure 2e), we consider the influence resulting from the gravity. Based on the above analyses, the force balance of the oil/water separation behavior could be quantitatively constructed, i.e., the Lucas–Washburn equation:[23]

$$\frac{2\sigma\cos\theta_0}{r_{equ}} = \frac{\varepsilon\mu}{K}H\frac{dH}{dt} + \rho gH \quad (3)$$

in which ρ and g are the density of the oil and the acceleration of gravity, respectively. Taking into consideration the boundary condition, i.e., $H|_{t=0} = 0$, we get the analytical solution of eq 3

$$t = -\frac{H}{b} - \frac{a}{b^2}\ln\left(1 - \frac{bH}{a}\right) \quad (4)$$

denoting $a = (K/\varepsilon\mu)(2\sigma\cos\theta/r_{equ})$ and $b = \rho g(K/\varepsilon\mu)$ as two coefficients. By employing the method of least-squares, we can determine the values of a and b. As can be seen in Figure 2e, $H(t)$ can be successfully described by eq 4 values were determined to be 1.83×10^{-5} and 9.0×10^{-4} m/s, respectively, for P2Bs, whereas $a = 1.0 \times 10^{-5}$ and $b = 2.17 \times 10^{-4}$ m/s for P3Bs. Moreover, it is supposed that the absorbed oil is uniformly distributed in the fiber, then the oil absorption quality could be estimated as follows:

$$Q(t) = \pi R^2\varepsilon\rho H(t) \quad (5)$$

DOI: 10.1021/acssuschemeng.8b03305
ACS Sustainable Chem. Eng. 2018, 6, 12580–12585

in which R is the radius of the fiber, and the rise height $H(t)$ is obtained using the aforementioned eq 4. Comparisons between the experimental and theoretical results are shown in Figure 2f, which indicates that our theoretical analyses are consistent with the experimental measurements. Herein, $\pi R^2 \varepsilon \rho$ were determined to be 6.5×10^{-3} and 1.1×10^{-2} kg/m, respectively, for P2Bs and P3Bs.

Figure 2g shows the saturated adsorption capacities of P2Bs and P3Bs for different oils and organic solvents. With regard to each kind of oil or organic solvent, the saturated adsorption capacity of P3Bs is larger than that of P2Bs. It means that P3Bs has the better saturated adsorption capacity due to its higher porosity. Moreover, all α values of P3Bs are more than 102% and the maximum value is 297% for silicone oil, which are related to liquid density and viscosity.

Continuous Oil−Water Separation Capability. Figure 3 shows the oil spill was pumped out to the collecting vessel. After pumping, the oil with water was in the collecting vessel for P2Bs (Figure 3c), which reveals that the low oil/water separation efficiency. In contrast, for P3Bs, cyclohexane was collected completely from the water surface after 15 s, and no water was observed in the collection vessel (Figure 3f and Move S5). Such self-controlled behavior means that a small piece of P3Bs can collect a large area of floating oil easily and quickly. This result demonstrates P3Bs is a promising material for continuous oil−water separation.

CONCLUSION

In summary, porous HDPE with excellent hydrophobicity and high absorption capacity was developed by an easy peeling method. The results demonstrate that peeling HDPE with villus-like structure on the surface can selectively collect oils and organic solvents from water. In addition, peeling HDPE can achieve continuous oil−water separation, thus breaking the limitation of the absorption capacity of sorption materials. Due to the continuous and solvent-free preparation, good commercial availability of raw materials, great potential for practical application, peeling HDPE reported might be a promising candidate to clean up oil spills and chemicals leaks.

ASSOCIATED CONTENT

Supporting Information

The Supporting Information is available free of charge on the ACS Publications website at DOI: 10.1021/acssuschemeng.8b03305.

Skin-peeling process as well as SEM images of P2Bs (PDF)

Video showing the absorption and removal of cyclohexane from water surface by P2Bs, video showing the absorption and removal of chloroform under water by P2Bs, video showing the absorption and removal of cyclohexane from water surface by P3Bs, video showing the absorption and removal of chloroform under water by P3Bs, and video showing an external pumping on P3Bs to realize the continuous collection of oil spills in situ from the water surface (ZIP)

AUTHOR INFORMATION

Corresponding Author

*X. Liu. Email: xianhu.liu@zzu.edu.cn.

ORCID

Xianhu Liu: 0000-0002-4975-3586

Hu Liu: 0000-0003-3840-8135

Zhanhu Guo: 0000-0003-0134-0210

Notes

The authors declare no competing financial interest.

ACKNOWLEDGMENTS

We express our great thanks to the 111 project (D18023), National Natural Science Foundation of China (51803190, 11432003, 11572290) and National Key Research and Development Program of China (2016YFB0101602) as well as the University Key Research Project of Henan Province (18A430031) for financial support.

REFERENCES

(1) Zhu, Q.; Chu, Y.; Wang, Z. K.; Chen, N.; Lin, L.; Liu, F.; Pan, Q. Robust Superhydrophobic Polyurethane Sponge as a Highly Reusable Oil-absorption Material. *J. Mater. Chem. A* **2013**, *1*, 5386−5393.

(2) Bi, H.; Xie, X.; Yin, K.; Zhou, Y.; Wan, S.; He, L.; Xu, F.; Banhart, F.; Sun, L.; Ruoff, R. S. Spongy Graphene as a Highly Efficient and Recyclable Sorbent for Oils and Organic Solvents. *Adv. Funct. Mater.* **2012**, *22*, 4421−4425.

(3) Zhu, Q.; Pan, Q.; Liu, F. Facile Removal and Collection of Oils from Water Surfaces Through Superhydrophobic and Superoleophilic Sponges. *J. Phys. Chem. C* **2011**, *115*, 17464−17470.

(4) Zhang, J.; Seeger, S. Superhyrophobic Materials: Polyester Materials with Superwetting Silicone Nanofilaments for Oil/Water Separation and Selective Oil Absorption. *Adv. Funct. Mater.* **2011**, *21*, 4699−4704.

(5) Wang, Y.; Wang, B.; Wang, J.; Ren, Y.; Xuan, C.; Liu, C.; Shen, C. Superhydrophobic and Superoleophilic Porous Reduced Graphene Oxide/Polycarbonate Monoliths for High-efficiency Oil/water Separation. *J. Hazard. Mater.* **2018**, *344*, 849−856.

(6) Zhang, A.; Chen, M.; Du, C.; Guo, H.; Bai, H.; Li, L. Poly(dimethylsiloxane) Oil Absorbent with a Three-dimensionally Interconnected Porous Structure and Swellable Skeleton. *ACS Appl. Mater. Interfaces* **2013**, *5*, 10201−10206.

(7) Sun, S.; Zhu, L.; Liu, X.; Wu, L.; Dai, K.; Liu, C.; Shen, C.; Guo, X.; Zheng, G.; Guo, Z. Superhydrophobic Shish-kebab Membrane with Self-cleaning and Oil/Water Separation Properties. *ACS Sustainable Chem. Eng.* **2018**, *6*, 9866−9875.

(8) Liu, X.; Pan, Y.; Zheng, G.; Liu, H.; Chen, Q.; Dong, M.; Liu, C.; Zhang, J.; Wang, N.; Wujcik, E. K.; Li, T.; Shen, C.; Guo, Z. Overview of the Experimental Trends in Water-Assisted Injection Molding. *Macromol. Mater. Eng.* **2018**, *303*, 1800035.

(9) Pan, Y.; Guo, X.; Zheng, G.; Liu, C.; Chen, Q.; Shen, C.; Liu, X. Shear-Induced Skin-Core Structure of Molten Isotactic Polypropylene and the Formation of β-Crystal. *Macromol. Mater. Eng.* **2018**, *303*, 1800083.

(10) Zhang, F.; Liu, X.; Zheng, G.; Guo, Z.; Liu, C.; Shen, C. Facile Route to Improve the Crystalline Memory Effect: Electrospun Composite Fiber and Annealing. *Macromol. Chem. Phys.* **2018**, *219*, 1800236.

(11) Liu, X.; Lian, M.; Pan, Y.; Wang, X.; Zheng, G.; Liu, C.; Schubert, D. W.; Shen, C. An Alternating Skin-Core Structure in Melt Multi-Injection-Molded Polyethylene. *Macromol. Mater. Eng.* **2018**, *303*, 1700465.

(12) Wang, X.; Pan, Y.; Qin, Y.; Voigt, M.; Liu, X.; Zheng, G.; Chen, Q.; Schubert, D. W.; Liu, C.; Shen, C. Creep and Recovery Behavior of Injection-molded Isotactic Polypropylene with Controllable Skin-core Structure. *Polym. Test.* **2018**, *69*, 478−484.

(13) Lu, X.; Zhang, C.; Han, Y. Low-density Polyethylene Superhydrophobic Surface by Control of Its Crystallization Behavior. *Macromol. Rapid Commun.* **2004**, *25*, 1606−1610.

(14) Erbil, H. Y.; Demirel, A. L.; Avci, Y.; Mert, O. Transformation of a Simple Plastic into a Superhydrophobic Surface. *Science* **2003**, *299*, 1377−1380.

DOI: 10.1021/acssuschemeng.8b03305
ACS Sustainable Chem. Eng. 2018, 6, 12580−12585

(15) Wang, Y.; Liu, X.; Lian, M.; Zheng, G.; Dai, K.; Guo, Z.; Liu, C.; Shen, C. Continuous Fabrication of Polymer Microfiber Bundles with Interconnected Microchannels for Oil/water Separation. *Appl. Mater. Today* **2017**, *9*, 77−81.
(16) Liu, Z.; Liu, X.; Zheng, G.; Dai, K.; Liu, C.; Shen, C.; Yin, R.; Guo, Z. Mechanical Enhancement of Melt-stretched β-nucleated Isotactic Polypropylene: The Role of Lamellar Branching of β-crystal. *Polym. Test.* **2017**, *58*, 227−235.
(17) Sun, X.; Cao, Z.; Bao, R.; Liu, Z.; Xie, B.; Yang, M.; Yang, W. A Green and Facile Melt Approach for Hierarchically Porous Polylactide Monoliths Based on Stereocomplex Crystallite Network. *ACS Sustainable Chem. Eng.* **2017**, *5*, 8334−8343.
(18) Niu, B.; Chen, J.; Chen, J.; Ji, X.; Zhong, G.; Li, Z. Crystallization of Linear Low Density Polyethylene on in situ Oriented Isotactic Polypropylene Substrate Manipulated by Extensional Flow Field. *CrystEngComm* **2016**, *18*, 77−91.
(19) Liu, X.; Dai, K.; Hao, X.; Zheng, G.; Liu, C.; Schubert, D. W.; Shen, C. Crystalline Structure of Injection Molded β-Isotactic Polypropylene: Analysis of the Oriented Shear Zone. *Ind. Eng. Chem. Res.* **2013**, *52*, 11996−12002.
(20) Pan, Y.; Liu, X.; Shi, S.; Liu, C.; Dai, K.; Yin, R.; Schubert, D. W.; Zheng, G.; Shen, C. Annealing Induced Mechanical Reinforcement of Injection Molded iPP Parts. *Macromol. Mater. Eng.* **2016**, *301*, 1468−1472.
(21) Jiang, J.; Liu, X.; Lian, M.; Pan, Y.; Chen, Q.; Liu, H.; Zheng, G.; Guo, Z.; Schubert, D. W.; Shen, C.; Liu, C. Self-reinforcing and Toughening Isotactic Polypropylene via Melt Sequential Injection Molding. *Polym. Test.* **2018**, *67*, 183−189.
(22) Hyväluoma, J.; Raiskinmäki, P.; Jäsberg, A.; Koponen, A.; Kataja, M.; Timonen, J. Simulation of Liquid Penetration in Paper. *Phys. Rev. E* **2006**, *73*, 036705.
(23) Bacri, L.; Brochard-Wyart, F. Droplet Suction on Porous Media. *Eur. Phys. J. E: Soft Matter Biol. Phys.* **2000**, *3*, 87−97.

DOI: 10.1021/acssuschemeng.8b03305
ACS Sustainable Chem. Eng. 2018, 6, 12580−12585